

Investigation of Electrical Signals in the Brain of People with Autism Using Effective Connectivity Network

Abstract

Unlike other functional integration methods that examine the relationship and correlation between two channels, effective connection reports the direct effect of one channel on another and expresses their causal relationship. In this article, we investigate and classify electroencephalographic (EEG) signals based on effective connectivity. In this study, we leverage the Granger causality (GC) relationship, a method for measuring effective connectivity, to analyze EEG signals from both healthy individuals and those with autism. The EEG signals examined in this article were recorded during the presentation of abstract images. Given the nonstationary nature of EEG signals, a vector autoregression model has been employed to model the relationships between signals across different channels. GC is then used to quantify the influence of these channels on one another. Selecting regions of interest (ROI) is a critical step, as the quality of the time periods under consideration significantly impacts the outcomes of the connectivity analysis among the electrodes. By comparing these effects in the ROI and various areas, we have distinguished healthy subjects from those suffering from autism. Furthermore, through statistical analysis, we have compared the results between healthy individuals and those with autism. It has been observed that the causal relationship between these two hemispheres is significantly weaker in healthy individuals compared to those with autism.

Keywords: Autism, electroencephalographic signal, effective connectivity, Granger causality

Submitted: 02-Mar-2024

Revised: 22-Apr-2024

Accepted: 03-May-2024

Published: 06-Aug-2024

Introduction

Autism spectrum disorder (ASD) is a set of clinical presentations that emerge due to neurodevelopmental disorders. Symptoms of ASD are related to social communication, imagination, and behavior. Accurate and timely diagnosis of ASD can significantly improve the quality of life for individuals with ASD.^[1] According to recent studies in the United States, 1 in 68 children are diagnosed with this disorder, and its prevalence is five times higher in boys than in girls (1 case in every 48 boys against 1 case in every 189 girls).

There is a hypothesis suggesting that ASDs are linked to abnormal neural connectivity.^[2] However, measuring this connectivity in practice presents challenges. Therefore, to assess the validity of this hypothesis, a range of brain imaging modalities and multiple methods for calculating connectivity are utilized.

This is an open access journal, and articles are distributed under the terms of the Creative Commons Attribution-NonCommercial-ShareAlike 4.0 License, which allows others to remix, tweak, and build upon the work non-commercially, as long as appropriate credit is given and the new creations are licensed under the identical terms.

For reprints contact: WKHLRPMedknow_reprints@wolterskluwer.com

Currently, electroencephalographic (EEG) signals are considered reliable tools for identifying and diagnosing abnormal symptoms and diseases.^[3-5] Experts are attempting to develop diagnostic biomarkers capable of differentiating between the wave patterns of healthy individuals and those with autism.

The connectivity of brain regions provides such a concise report on the activity of nerve cells that its description of the relationships between different brain regions is a very important subject in neuroscience. Interactions between specialized areas of brain function are crucial for normal brain operation. EEG is a suitable technique for recording these interactions because it measures the entire brain's activity within milliseconds. However, EEG records the activity of the cortex via the scalp in such a way that the activity of a primary source in the cortex may be recorded by more than one sensor (EEG electrode).

Advances in research in network analysis, time-series analysis, and biomedical

How to cite this article: Bahrami F, Taghizadeh M, Shayegh F. Investigation of electrical signals in the brain of people with autism using effective connectivity network. *J Med Sign Sens* 2024;14:24.

Farzaneh Bahrami¹,
Maryam
Taghizadeh¹,
Farzaneh Shayegh²

¹Faculty of Technology and
Engineering, Shahrekord
University, Shahrekord, Iran,

²Electrical and Computer
Engineering, Isfahan University
of Technology, Isfahan, Iran

Address for correspondence:

Dr. Maryam Taghizadeh,
Shahrekord University,
Shahrekord, Iran.

E-mail: m_taghizadeh@sku.ac.ir

Access this article online

Website: www.jmssjournal.net

DOI: 10.4103/jmss.jmss_15_24

Quick Response Code:



engineering have facilitated the extraction of brain network structures based on EEG signals. By assuming various models for EEG signals, connectivity can be defined from multiple perspectives. There are two primary definitions of brain connectivity: functional connectivity and effective connectivity.^[6]

Functional connectivity is defined as the temporal correlation between spatially distinct events. The calculation of functional connectivity involves checking the symmetrical correlation between the active regions of the brain. In other words, if there is a statistical relationship between the recorded activities of these regions, they are said to have functional connectivity, indicating that these regions are components of a network. Functional connectivity reflects the similarity and/or synchronous activity of brain regions, regardless of the source of this similarity.^[7] That is, functional connectivity cannot recognize situations in which two regions are not directly interconnected but exhibit similar behavior due to a common source in the brain.

From the standpoint of connectivity measurement, the importance of using EEG lies in capturing the dynamics of brain networks on a timescale of <1 s. Its temporal resolution enables the examination of brain activity across large networks. However, the low spatial resolution of EEG increases the risk of false positives due to volume conduction and artificial connections. To mitigate these drawbacks, it is possible to search for transient changes in brain sources by employing isolation and localization techniques. This guides researchers toward connectivity metrics that incorporate source reconstruction and their causal effects. It should be noted that the source localization (reconstruction) problem can never be completely resolved. However, there has been very exciting and progressive research in this field. A key alternative often useful in the study of connectivity is effective connectivity, as opposed to functional connectivity. Unlike functional connectivity, which determines statistical dependencies between neural signals without considering directed interactions (symmetric), effective connectivity assesses the direct influence of one brain region on another (asymmetric).

In other words, effective connectivity quantifies the extent to which an event in one region precipitates changes in the activity of other regions. The influence of one EEG channel on others can be ascertained through dynamic causal modeling (DCM). This model, stemming from a channel integration model, encapsulates the mechanisms of neural activities. Here, the objective is to identify which brain structures within a functional network causally impact other network components. In addition, the multichannel autoregressive (AR) model (vector autoregression [VAR] model) serves as another suitable model for synchronizing EEG signals.^[8] This model is

constructed using a two-variable AR model, also known as a VAR model, which includes both time series in their past values. The noise variance for the first channel in the AR model is juxtaposed with the noise variance in the VAR model, comprising both the first and second channels. If the variance in the single-channel model is significantly reduced in comparison to the two-channel model, it suggests that the second time series exerts a causal influence on the first series. The principal advantage of this criterion is its interpretability within the context of both random and deterministic models.

In 2015, a comparative study was conducted in the field of patterns related to brain connections on healthy people and people with autism.^[1] In this study, a screening strategy is proposed to distinguish individuals with ASD from healthy individuals. Connection patterns are estimated based on EEG data collected from 8 brain regions under different psychological conditions. EEG data from 12 healthy individuals and 6 autistic children (aged 7–10 years) in resting state with eyes open and eyes closed, as well as when people were exposed to emotional faces (happy, sad, and calm), had been collected. The performance of the proposed system is evaluated separately in each mental state. Higher detection rates are provided by using functional connectivity feature extraction than other feature extraction methods. In autistic children, understanding of emotional faces is disturbed. Therefore, the stimulus-processing speed decreases. This may be due to changes in the functional and effective structure of the brain, which has been shown using EEG studies.^[9]

In 2015, Klamer *et al.* were able to diagnose a group of individuals with epilepsy by extracting characteristics from EEG signals.^[10] In addition, in the same year, further research led to the classification of 30 children, who had been definitively diagnosed with autism, into various categories, including mild, moderate, and severe ASD.^[11] In recent years, the diagnosis of autism disorder through feature extraction and the classification of EEG signals from both healthy individuals and those with autism has been conducted.

In this research, both causal relationships (effective connectivity measures) and correlations between two brain regions (functional connectivity measures) have been utilized to diagnose autism by analyzing EEG signals. The following points are considered when calculating the effective connectivity measures:

- In this research, scalp EEG signals are utilized without the application of any source localization algorithm. Instead, to account for the limitations of scalp EEG signals and to extract actual causalities in the brain, effective connectivity measures are employed
- Calculating effective connectivity measures necessitates a predefined physiological EEG generative model; without it, the results would lack significance

- In the current study, the Granger causality (GC) method in the time domain is employed to measure the effective connectivity of healthy and autistic brains. This research differs from previous studies in this field due to the reduced computational load, thereby simplifying the diagnosis of the disorder
- The dataset used in this article includes 9 subjects with autism and 7 healthy subjects, with the EEG signal of each individual recorded using 129 channels. This high number of channels creates a dense record of scalp activity, from which more information can be gleaned
- The model assumed for measuring GC is a VAR model that accounts for noise. Consequently, in the preprocessing stage, the step of removing noise and specific signal bands is omitted, which reduces the time required for preprocessing. In addition, this allows for the analysis of all frequencies.

The structure of the article is as follows: Section “Materials and Methods” explains the proposed method and the properties of the data. Section “Implementation” explains the implementation of the proposed method. Section “Results” presents the results of applying the method. Finally, Section “Conclusion” discusses the conclusions of our proposed method and compares the data of healthy individuals and those with autism.

Materials and Methods

The human brain is a complex network consisting of several regions through which information is transferred from one region to another. By measuring brain connectivity and extracting the resulting features, we can define a network known as a functional integration network. The measurement of the connectivity of brain regions is divided into three categories: structural connectivity, functional connectivity, and effective connectivity.^[12]

Unlike the symmetric nature of functional connectivity, effective connectivity accounts for the asymmetric causal dependencies. The aim of effective connectivity measures is to identify which brain structures within a network causally influence other elements during rest or cognitive tasks. Effective connectivity is determined using various methods, including DCM,^[13] structural equation modeling,^[14] and GC.

In this article, we utilize GC to calculate the relationships between electrodes at various points on the scalp and ultimately investigate their role in the diagnosis of ASD.

Other studies have used other methods of functional connectivity or effective connectivity in order to diagnose autism directly. Predictive and improved methods of multivariate realizations have been used to infer GC among EEG signals. Due to the high temporal resolution, EEG data recorded from continuous neural activity are suitable for GC analysis.^[15] In this research, the GC method has been used directly in the time domain, so that by reducing

the calculations, the diagnosis of the disorder can be done more easily.

This analysis is performed on scalp EEG signals by measuring the correlation of head points. The calculation of GC in time series depends on linear methods. Linearization models should be used in nonlinear and unstable EEG signals. GC is a method to infer certain types of causal relationships between random variables in order to reduce the error in predictions.

The block diagram of the proposed method is shown in Figure 1.

Dataset

The dataset utilized in this research includes EEG signals from 9 subjects diagnosed with autism and 7 healthy subjects. The subjects were children aged between 26.6 and 98.7 months. The EEG signals were recorded using 129 high-density channels at a sampling frequency of 256 Hz with geodesic grids. Data recording occurred while the participants watched silent videos featuring the movement of soap bubbles and other abstract images on a computer.^[16]

The EEG recording lasted between 2 and 6 min, varying according to each child’s adaptation to the conditions. Sedation was not employed for electrode placement or during the EEG recording. The EEG signals were amplified using a NetAmps 300 amplifier. All data were collected in compliance with the guidelines set by the Institutional Review Board of the University of California. Written consent was obtained from the parents of the participants before commencing the study activities. Detailed information about the subjects is presented in Table 1.

Data preparation

In the preprocessing step, the data were first normalized between 0 and 1. Subsequently, some channels identified as malicious were removed. The voltage values in certain channels exhibited a significant numerical difference compared to others; after normalization, some channels attained a value of one across all 30,000 samples. Indeed, the uniform potential (value of one) along the entire length of the channel poses challenges in variance calculation.

$$\mu = \frac{1}{N-1} \sum_{i=1}^{N-1} x_i$$

Here, μ represents the average value of the channel and N is the total number of samples.

$$\text{var} = \frac{1}{N-1} \sum_{i=1}^{N-1} |x_i - \mu|^2$$

This issue is predominantly observed in the data from electrodes 125 to 129, which are considered destructive channels and thus removed from the measurement. Consequently, 124 channels were utilized for testing and

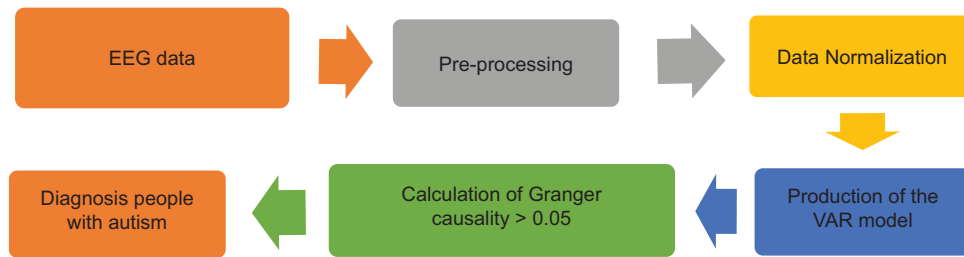


Figure 1: The block diagram of the proposed method. EEG: Electroencephalographic; VAR: Vector autoregression

Table 1: Detailed information of the dataset used in this study

Group	Age (months)	Site	Gender	Meds	Genetics	Epilepsy	Verbal Developmental Quotient (VDQ)	Nonverbal Developmental Quotient (NVDQ)
ASD	61.2	UCLA	Male	Focalin, risperidone	N/A	no	51	48
ASD	26.6	UCLA	Male	none	N/A	no	19	45
ASD	39.3	UCLA	Male	none	N/A	no	33	46
ASD	63	UCLA	Male	none	N/A	no	43	41
ASD	28.8	UCLA	Male	none	N/A	no	28	52
ASD	53.2	UCLA	Female	risperidone	N/A	no	56	51
ASD	48.6	UCLA	Male	none	N/A	no	17	49
ASD	32.3	UCLA	Male	none	N/A	no	25	43
ASD	58.5	UCLA	Female	Zoloft	N/A	no	103	74
ASD	98.7	UCLA	Male	melatonin	N/A	no	21	50
TD	57	UCLA	Female	none	N/A	no	122	94
TD	54	UCLA	Male	none	N/A	no	98	97
TD	29	UCLA	Male	none	N/A	no	131	157
TD	55	UCLA	Male	none	N/A	no	140	107
TD	38.8	UCLA	Female	none	N/A	no	145	149
TD	43.8	UCLA	Male	none	N/A	no	109	115
TD	40.8	UCLA	Male	none	N/A	no	141	113
TD	59.6	UCLA	Female	none	N/A	no	127	103
TD	59.6	UCLA	Male	none	N/A	no	112	117

calculating GC. Furthermore, to enhance accuracy, a window comprising 1000 time points – equivalent to 4 s of data – was randomly selected. This dataset is used in Ardakani *et al.*'s study.^[17] The preprocessing process in each study is tailored to the chosen method for analyzing the recorded data. This may include applying intermediate filters to the data, altering the sampling frequency, changing the reference electrode, removing harmful channels, extracting principal components, and deciding whether to retain or discard these components. In the preprocessing stage, these steps are applied at the researchers' discretion. In this study, we employed data normalization, removed destructive channels, and applied a low-pass filter.

Vector autoregression modeling

The GC framework is indeed a method for quantifying the influence of a time series on another. The foundation of GC is the AR model applied to individual channels. For a given channel x , a p -th order AR model can be represented by the following Eq. (1):

$$x(t) = \sum_{l=1}^p A_{1l} x(t-l) + \eta_x(t) \quad (1)$$

Here, p is the model order, indicating the number of past samples on which the signal depends. Here, η_x represents noise with zero mean and σ_1^2 variance.^[18] A_{1l} is the dependency coefficient of l -th past sample time to current time.

In general, selecting the appropriate coefficients A and noise variance $\sigma_1^2 = \text{Var}(\eta_x(t))$ contributes to the stability of the model. Typically, in AR modeling, the mean and variance of the noise remain constant over time. An AR process will be stable if the matrix of coefficients is invertible:

$$\det(I-A) \neq 0$$

Extending this single-channel model to a two-variable AR model, referred to as a VAR model, both time series could be related to each other by their past values. The same formulation could be written for the VAR model of the x and y channels.

$$\begin{cases} x(t) = \sum_{l=1}^p A_{11} x(t-l) + A_{12} y(t-l) + e_x(t) \\ y(t) = \sum_{l=1}^p A_{21} x(t-l) + A_{22} y(t-l) + e_y(t) \end{cases} \quad (2)$$

where e_x and e_y are the zero-mean noises relevant to the channels, with respective variances σ_x^2 and σ_y^2 variances. σ_{xy} is the covariance of e_x and e_y . After calculating the AR and VAR models for a channel x and y , the noise variance of the AR model for the x -channel (σ_1^2) is compared with its corresponding noise variance in the VAR model (σ_x^2). If it is significantly reduced, it indicates that the y time series has a causal effect on the x time series.

Two important parameters, whose proper estimation is crucial for creating an optimal regression model, are the model coefficients and the noise variance. The least squares method is commonly used to estimate the parameters of the AR and VAR models.^[19] Including more variables than necessary can yield misleading results. In other words, the model order must be selected accurately. Thus, the objective is to determine the model order that minimizes a given criterion. In this study, the Akaike information criterion (AIC) method is employed due to its effectiveness; the most precise model is the one with the lowest AIC value. Moreover, the model order is influenced by the sampling quantity. Experiments suggest that for EEG data with a sampling rate of 256 Hz, the optimal model order ranges between 20 and 30.^[20] In this study, due to the variance between data in healthy and autism states, a range of 1–30 has been considered for the model order. The AIC is calculated for each potential model order. Ultimately, the order that yields the minimum AIC value from these 30 calculations is chosen as the most appropriate for the model.

Compatibility percentage

To evaluate the performance of the regression models, the compatibility percentage is assessed. This metric demonstrates what percentage of the original data's correlation is accurately reproduced in the model-based simulated data. For this purpose, both the original and simulated signals, as well as their autocorrelation functions, have been calculated for various delay values.^[21] Consequently, the compatibility percentage is defined as shown in Eq. 3.

$$PC = \left(1 - \frac{\|R_s - R_r\|}{\|R_r\|} \right) \times 100 \quad (3)$$

Here, R_s is the correlation matrix of the modeled data and R_r is the correlation matrix of the original data. A PC value close to 100% indicates that the modeled data closely resemble the original, thereby validating the success of the modeling. Conversely, a PC value near zero signifies

a failure in the modeling process. Ideally, the PC should be >85% for the model to be considered successful.

In this research, efforts have been made to maximize the compatibility percentage through preprocessing. Subsequently, based on the VAR coefficients of such a model, the effective connectivity of EEG channels is determined. These connectivity values are anticipated to serve as significant features for the detection of autism.

Regression model performance accuracy test

To evaluate the performance of the regression model within the written program, an AR model was generated using random data.^[22] For instance, two coefficients, $a = -0.25$ and $b = 0.75$, were chosen for the delay values $P = 1$ and $P = 2$, respectively. In addition, random Gaussian white noise was generated. These parameters were used to create a random channel, which was then incorporated into the program code. Upon executing the program, reasonable estimates for the coefficients a and b were obtained. For a two-channel model, the coefficients at each order of the P model correspond to a 2×2 matrix in the following form:

$$\beta = \begin{bmatrix} A_{11} & A_{12} \\ A_{21} & A_{22} \end{bmatrix}$$

Due to the independence of the channels, the coefficients A_{21} and A_{12} are close to zero in order to check the causal relationships.

Calculation of effective connection

In the proposed method, the AR and VAR models in the time domain are utilized to calculate the GC.^[23] As outlined in the previous section, two stages of modeling are undertaken:

- Modeling single-channel signals (as per Eq. [1]), which have noise variances ranging from σ_1^2 to σ_{124}^2
- Where pairs of channels are modeled together with the aim of measuring all possible connectivities between brain regions. For each pair (channels i and j), a covariance matrix is constructed as follows:

$$\Sigma_{noise} = \begin{bmatrix} \sigma_{ii} & \sigma_{ij} \\ \sigma_{ij} & \sigma_{jj} \end{bmatrix}$$

To interpret an effect from channel j toward channel i , the following two conditions must be met:

- 1) $\sigma_i > \sigma_{ii}$
- 2) be the matrix of coefficients $A > 0$ for $1 \in \{1 \dots p\}$.

Accordingly, GC or the impact of channel j on channel i is defined as follows:

$$F_{j \rightarrow i} = \ln \frac{\sigma_i}{\sigma_{ii}} \quad (4)$$

As a result of calculating σ_{ii} , a 124×124 GC connectivity matrix is created, whose diagonal elements are undefined.

Thresholding

After estimating GC as the F defined in Eq. 4, it is necessary to discard some small values. These may not indicate actual connectivity but rather arise from measurement noise and errors in covariance estimation. Therefore, analyzing confidence intervals and performing statistical assessments for threshold selection are crucial in determining information flow or causality in the brain.^[24,25] The concept of a normal distribution and the null hypothesis (H_0) can be applied. The null hypothesis posits that there is no causal connectivity between two brain regions (no information flow). Assuming a normal distribution for GC values, a threshold can be established for each alpha value to achieve a significant level for the correct rejection of the null hypothesis. According to a rule for conducting a statistical hypothesis test based on an observed value, the null hypothesis is rejected when the probability of H_0 for the observed value is $< \alpha$, as illustrated in Figure 2.^[26]

- H_0 (null hypothesis): Also known as the statistical or null hypothesis, it posits the absence of a relationship, effect, or connectivity between brain regions. It is the default assumption that there is no effect or difference
- H_1 (alternative hypothesis): This hypothesis suggests the presence of a relationship, effect, or connectivity between brain regions. It is considered when there is sufficient evidence to reject the null hypothesis.

In hypothesis testing, you compare your data against the predictions made by H_0 . If the data significantly deviate from what is expected under H_0 , you may reject the null hypothesis in favor of H_1 , suggesting that your findings are not due to random chance.

Threshold selection

Finally, GC values are calculated for all valid 124 channels of each subject. Subsequently, it is necessary to exclude the small GC values. To determine the appropriate threshold, considering the null hypothesis H_0 , histograms of GC values for both healthy and autistic subjects are constructed, as depicted in Figure 3. The dispersion of GC values among healthy individuals and those with autism has been analyzed. Given the similarity between both groups in the range of 0–0.05, a threshold of 0.05 has been established for further examination. Therefore, GC values > 0.05 have been scrutinized. By setting this threshold, a subset of correlations between channels and, consequently, certain brain regions can be compared between healthy individuals and those with autism. The investigations reveal that the graphs representing healthy individuals are consistent within the group, and similarly, the graphs for individuals with autism are consistent within their group.

As mentioned in Section “Thresholding,” the rejection of null hypothesis for healthy people is shown in Figure 4.

In the following, the results, which include a 124×124 matrix for each data, are analyzed to compare healthy and autistic people.

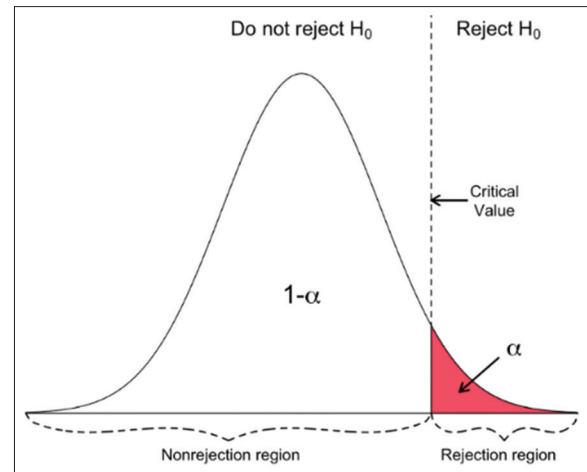


Figure 2: Statistical assumption test

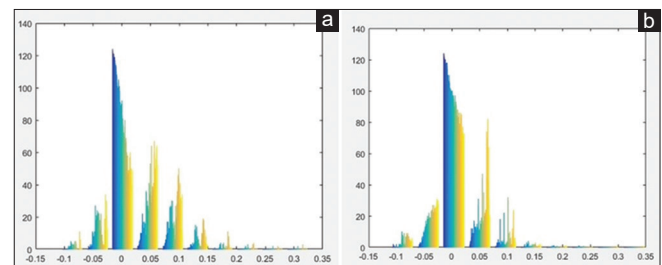


Figure 3: Histogram chart of Granger causality values > 0.05 (a) in healthy people, (b) in people with autism

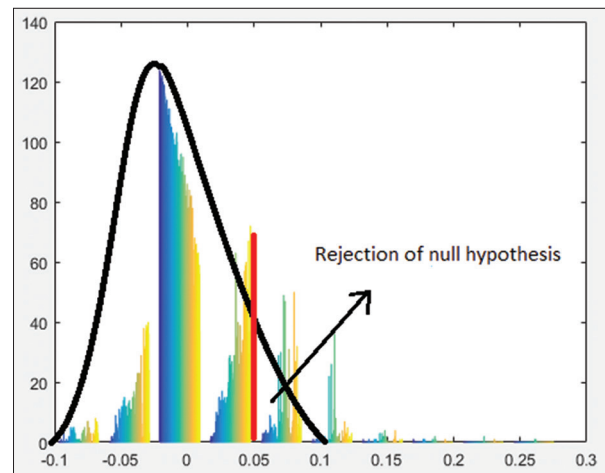


Figure 4: Determining the statistical test threshold in healthy people

Implementation

As mentioned in Section “Data preparation,” the data contains 124 channels; each channel represents a time series (124 EEG channels with 1000 time samples in a signal window). By applying AR and VAR models to single channels and channel pairs of windowed EEG signals, we obtain 124×124 connectivity values for each window, which are used to measure their causal effects.

The results are examined from two perspectives:

- Different regions of the brain are analyzed, with some designated as regions of interest (ROIs)
- The effective connectivity originating from the ROI areas is statistically assessed to distinguish healthy individuals from those with autism.

Regions of interest description

Selecting ROIs is crucial to confine the spatial area and enhance accuracy in research. Each electrode, representing a brain region, is denoted by a number. Figure 5 schematically displays the 128 electrodes utilized for EEG recording. It is evident that the electrodes in the occipital region fall within the numerical range of 60–100. The electrodes numbered from 40 to 60 correspond to the left hemisphere and the lateral region. The regions responsible for language processing are situated on the left side of the brain, which is predominantly used by individuals to comprehend concepts. As previously mentioned, the EEG signals were recorded from individuals while they were observing soap bubbles. Consequently, it is anticipated that the occipital region, which is associated with vision processing, would exhibit increased connectivity with the left hemisphere. This type of connectivity is rational for comprehending the visual concepts being observed and is observed in both healthy and autistic subjects.

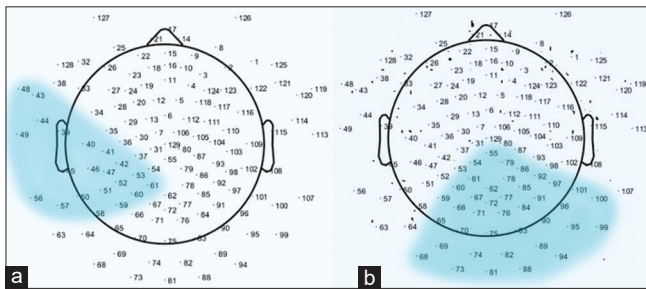


Figure 5: (a) Electrodes of the left lateral region, (b) electrodes of the occipital region

Regions of interest selection

As an example, matrices with GC values >0.05 for two subjects – one healthy and one with autism – are visualized in Figure 6. The GC values are color coded to enhance the visualization. A notable difference observed between the healthy subject and the subject with autism is the extent of brain region involvement and connectivity. As depicted in Figure 6a, in the subject with autism, all brain regions are engaged when viewing and processing the images of soap bubbles. For this reason, certain brain regions were examined more narrowly, and the ranges of 40–60 (left side area) and 100–120 (right side area) were selected as ROIs for this study. These areas are highlighted with red squares in Figure 6. To facilitate the visualization of effective connectivity within these ROIs, the electrodes are displayed in greater detail. In the subject with autism, Granger connectivity is present in the channels marked in yellow, with values approximately between 0.25 and 0.3. This level of connectivity is considerably lower in the healthy subject, with values ranging from 0.05 to 0.1. This indicates that, in healthy subjects, there is no significant causal connectivity between these two brain regions when observing soap bubbles as shown in Figure 6b. Although in Figure 6, only two subjects are compared, similar differences can be seen in all healthy/autism subjects. The statistical analysis of distinction of these two classes is given in the next section.

Results

Statistical analysis

Statistical inference is utilized to make decisions about an entire population based on information from one to two samples. Bar graphs are commonly employed to compare groups based on a qualitative variable. The values on the

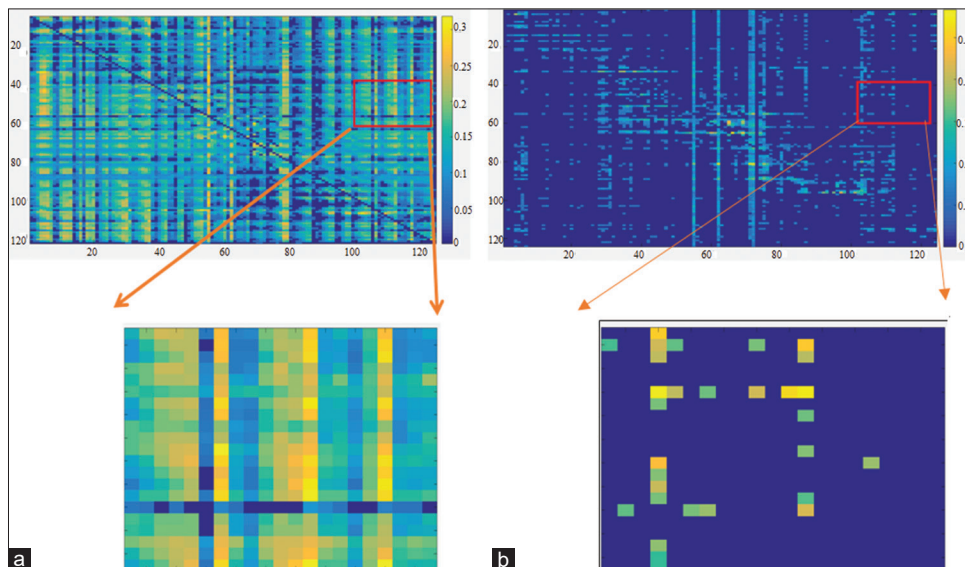


Figure 6: (a) Granger causality >0.05 in autistic people. (b) Granger causality >0.05 in healthy people

vertical axis of these charts typically represent counts of a qualitative variable or calculations of a statistical index for a quantitative variable. In this case, a bar chart is used to display the number of levels exceeding 0.05 in the GC matrix, facilitating a comparison between healthy individuals and those with autism. The vertical axis of the bar chart indicates the count of levels >0.05 in the GC matrix for channels 40–60 when connected to channels 100–120. As illustrated in Figure 7, the number of these regions in individuals with autism is nearly tenfold that in healthy individuals. Within this channel range, there are 21×21 potential effective connection patterns. Out of these 441 patterns, healthy individuals exhibit at most 50 effective connections. However, in the autism group, there are observed connections ranging from a minimum of 80 to a maximum of 430. Indeed, effective connectivity within this channel range is significantly greater in individuals with autism, indicating a higher degree of inter-channel influence. To differentiate these two groups

and compare outcomes, other statistical methods can also be employed.

The dispersion and distribution of Granger values across this range of channels, and their differences between healthy individuals and those with autism, were analyzed using a box plot. To thoroughly examine certain datasets, more information is required beyond central tendency measures such as the mean, median, and mode. A box plot provides insights into the spread of data values. The rectangle within the plot represents the interquartile range, encompassing the distribution between the 25th and 75th percentiles. The 10th percentile is the value below which x percent of the data falls. Thus, the middle 50% of the data lies between the 25th and 75th percentiles. The box plot results for the data pertaining to healthy and autistic individuals are depicted in Figure 8. According to the concepts discussed, the graphs labeled with numbers 1–7 correspond to healthy individuals, while those labeled 8–16 pertain to individuals with autism. As outlined in the previous section, the nonoverlapping box plots for the autistic group compared to those for the healthy group indicate a significant statistical difference between the two. Furthermore, a visual inspection of the graphs in Figure 8 reveals a clear distinction in the range of values between the datasets of healthy individuals and those with autism. The matrix values of effective connections for healthy individuals are predominantly centered around zero, whereas the box plots for individuals with autism demonstrate a broader dispersion of values within the effective connections matrix. The GC matrix is a 124×124 matrix. When setting a threshold with GC values >0.05 , all other values in the matrix are considered zero. It is observed that the number of GC values exceeding 0.05 is lower in healthy individuals compared to those with autism within the specified channel range. Consequently, for healthy groups, the median and the first and third

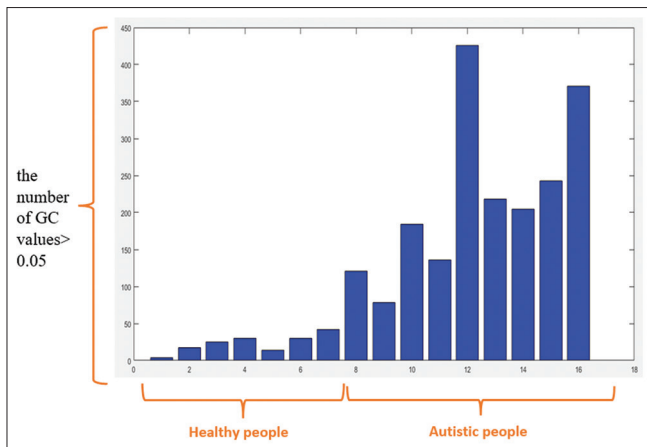


Figure 7: Bar graph of the number of Granger causality levels >0.05 . GC – Granger causality

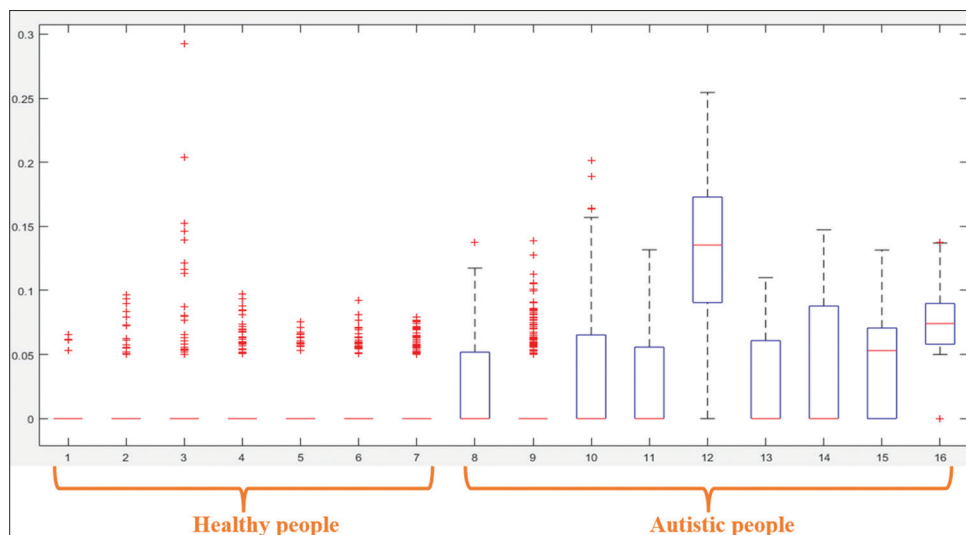


Figure 8: Graphic box of Granger value

quartiles are zero, with data points clustering closely between 0.05 and 0.1. In contrast, individuals with autism exhibit effective connectivity across most brain regions, with GC values >0.05 . This results in differing statistical values, including the median. In addition, in certain cases of autism, the Granger values approach 0.25, indicating a more extensive interconnection between channels in the left and right lateral areas of the brain.

Conclusion

In this study, the impact of brain region activity on one another for both healthy individuals and people with autism is investigated using the effective connectivity method (GC). As noted, the research involved calculations based on data from 9 individuals with autism and 7 healthy individuals, encompassing 124 channels recorded at a frequency of 256 Hz.

After normalizing the data and removing destructive channels as part of the preprocessing, the application of VAR models and a composite index like the GC index in the time domain enabled the evaluation of changes in brain connectivity among the participants. Following VAR modeling for channel pairs, the GC value for each model was calculated using the noise variance calculation method outlined in Formula 4. The GC index quantifies the influence of one brain channel on another.

Given the similarities between both groups in the range of 0–0.05 and the differences beyond 0.05, a threshold of 0.05 was established. For each dataset, an Excel file was generated containing the results for 124 channels. Essentially, there are 124×124 values representing the causal and unidirectional communication from row channels to column channels. Considering the channels' independence in effective connectivity, the principal diagonal – representing each channel's self-connection – is set to zero. Furthermore, in accordance with the GC threshold, values <0.05 are also zeroed in the matrix. Subsequent analysis of the left and right hemispheres revealed that the causal interactions between these hemispheres are significantly lower in healthy individuals compared to those with autism.

Acknowledgment

This research is supported by the Cognitive Sciences and Technologies Council, Tehran, Iran.

Financial support and sponsorship

This study is funded by the Cognitive Sciences and Technologies Council, Tehran, Iran.

Conflicts of interest

There are no conflicts of interest.

References

1. Lord C, Brugha TS, Charman T, Cusack J, Dumas G, Frazier T, *et al.* Autism spectrum disorder. *Nat Rev Dis Primers* 2020;6:5.
2. Carroll L, Braeutigam S, Dawes JM, Krsnik Z, Kostovic I, Coutinho E, *et al.* Autism spectrum disorders: Multiple routes to, and multiple consequences of, abnormal synaptic function and connectivity. *Neuroscientist* 2021;27:10-29.
3. Bronzino JD, Peterson DR. Principles of electroencephalography. In: *Biomedical Engineering Fundamentals*. 1st ed. Taylor and Francis Group: CRC Press; 2006. p. 445-56.
4. Shayegh F, Bellanger JJ, Sadri S, Amirfattahi R, Ansari-Asl K, Senhadji L. Analysis of the behavior of a seizure neural mass model using describing functions. *J Med Signals Sens* 2013;3:2-14.
5. Wijayanto I, Hartanto R, Nugroho HA. Quantitative analysis of inter- and intrahemispheric coherence on epileptic electroencephalography signal. *J Med Signals Sens* 2022;12:145-54.
6. Niso G, Bruña R, Pereda E, Gutiérrez R, Bajo R, Maestú F, *et al.* HERMES: Towards an integrated toolbox to characterize functional and effective brain connectivity. *Neuroinformatics* 2013;11:405-34.
7. Chiarion G, Sparacino L, Antonacci Y, Faes L, Mesin L. Connectivity analysis in EEG data: A tutorial review of the state of the art and emerging trends. *Bioengineering (Basel)* 2023;10:372.
8. Li P, Wang X, Li F, Zhang R, Ma T, Peng Y, *et al.* Autoregressive model in the LP norm space for EEG analysis. *J Neurosci Methods* 2015;240:170-8.
9. Ashwin E, Chapman E, Colle L, Baron-Cohen S. Impaired recognition of negative basic emotions in autism: A test of the amygdala theory. *Soc Neurosci* 2006;1:349-63.
10. Klamer S, Rona S, Elshahabi A, Lerche H, Braun C, Honegger J, *et al.* Multimodal effective connectivity analysis reveals seizure focus and propagation in musicogenic epilepsy. *Neuroimage* 2015;113:70-7.
11. Khosrowabadi R, Quek C, Ang KK, Wahab A, Chen SH. Dynamic screening of autistic children in various mental states using pattern of connectivity between brain regions. *Appl Soft Comput* 2015;32:335-46.
12. Yang M, Cao M, Chen Y, Chen Y, Fan G, Li C, *et al.* Large-scale brain functional network integration for discrimination of autism using a 3-d deep learning model. *Front Hum Neurosci* 2021;15:687288.
13. Friston KJ, Harrison L, Penny W. Dynamic causal modelling. *Neuroimage* 2003;19:1273-302.
14. Astolfi L, Cincotti F, Babiloni C, Carducci F, Basilisco A, Rossini PM, *et al.* Estimation of the cortical connectivity by high-resolution EEG and structural equation modeling: Simulations and application to finger tapping data. *IEEE Trans Biomed Eng* 2005;52:757-68.
15. Seth AK, Barrett AB, Barnett L. Granger causality analysis in neuroscience and neuroimaging. *J Neurosci* 2015;35:3293-7.
16. Frohlich J, Senturk D, Saravanapandian V, Golshani P, Reiter LT, Sankar R, *et al.* A quantitative electrophysiological biomarker of duplication 15q11.2-q13.1 syndrome. *PLoS One* 2016;11:e0167179.
17. Ardakani HA, Taghizadeh M, Shayegh F. Diagnosis of autism disorder based on deep network trained by augmented EEG signals. *Int J Neural Syst* 2022;32:2250046.
18. Bakhshayesh H, Fitzgibbon SP, Janani AS, Grummett TS, Pope KJ. Detecting connectivity in EEG: A comparative study of data-driven effective connectivity measures. *Comput Biol Med* 2019;111:103329.
19. Lawhern V, Hairston WD, McDowell K, Westerfield M,

- Robbins K. Detection and classification of subject-generated artifacts in EEG signals using autoregressive models. *J Neurosci Methods* 2012;208:181-9.
20. Delorme A, Mullen T, Kothe C, Akalin Acar Z, Bigdely-Shamlo N, Vankov A, *et al.* EEGLAB, SIFT, NFT, BCILAB, and ERICA: New tools for advanced EEG processing. *Comput Intell Neurosci* 2011;2011:130714.
 21. Mullen T. Source Information Flow Toolbox (SIFT): An Electrophysiological Information Flow Toolbox for EEGLAB Theoretical Handbook and User Manual. Department of Cognitive Science University of California, San Diego: Swartz Center for Computational Neuroscience and Institute for Neural Computation and Department of Cogn; 2010.
 22. Van Drongelen W. Signal Processing for Neuroscientists. Academic Press is an imprint of Elsevier: Academic press; 2018.
 23. Lima V, Dellajustina FJ, Shimoura RO, Girardi-Schappo M, Kamiji NL, Pena RF, *et al.* Granger causality in the frequency domain: Derivation and applications. *Rev Bras Ensino Fís* 2020;42:e20200007.
 24. Faes L, Porta A, Nollo G. Testing frequency-domain causality in multivariate time series. *IEEE Trans Biomed Eng* 2010;57:1897-906.
 25. Porta A, Guzzetti S, Furlan R, Gnecchi-Ruscone T, Montano N, Malliani A. Complexity and nonlinearity in short-term heart period variability: Comparison of methods based on local nonlinear prediction. *IEEE Trans Biomed Eng* 2007;54:94-106.
 26. Frick RW. Accepting the null hypothesis. *Mem Cognit* 1995;23:132-8.